© 2019. Published by The Company of Biologists Ltd | Development (2019) 146, dev177121. doi:10.1242/dev.177121

RESEARCH ARTICLE

Identification of the building blocks of ventricular septation in monitor lizards (Varanidae)

Jermo Hanemaaijer[1,*], Martina Gregorovicova[2,3,*], Jan M. Nielsen[4], Antoon F. M Moorman[1], Tobias Wang[5], R. Nils Planken[6], Vincent M. Christoffels[1], David Sedmera[2,3,‡] and Bjarke Jensen[1,‡]

ABSTRACT

Among lizards, only monitor lizards (Varanidae) have a functionally divided cardiac ventricle. The division results from the combined function of three partial septa, which may be homologous to the ventricular septum of mammals and archosaurs. We show in developing monitors that two septa, the 'muscular ridge' and 'bulbuslamelle', express the evolutionarily conserved transcription factors *Tbx5*, *Irx1* and *Irx2*, orthologues of which mark the mammalian ventricular septum. Compaction of embryonic trabeculae contributes to the formation of these septa. The septa are positioned, however, to the right of the atrioventricular junction and they do not participate in the separation of incoming atrial blood streams. That separation is accomplished by the 'vertical septum', which expresses *Tbx3* and *Tbx5* and orchestrates the formation of the electrical conduction axis embedded in the ventricular septum. These expression patterns are more pronounced in monitors than in other lizards, and are associated with a deep electrical activation near the vertical septum, in contrast to the primitive base-to-apex activation of other lizards. We conclude that evolutionarily conserved transcriptional programmes may underlie the formation of the ventricular septa of monitors.

KEY WORDS: Heart, Ventricular septum, Evolution, Lizard

INTRODUCTION

The evolution of land-living vertebrates was facilitated by the ability to breathe air with lungs (Perry and Sander, 2004). A dedicated vascular bed, the pulmonary circulation, enables the perfusion of the lungs by blood. The oxygenated blood of this circulation returns to the left side of the heart (Burggren and Johansen, 1986). However, the oxygen-rich blood from the lungs may mix with oxygen-poor blood returning from the systemic circulation if septal structures are absent in the ventricle of the heart. In mammals and in archosaurs (crocodylians and birds), the ventricle is divided into the left and right ventricle by a full ventricular septum (Poelmann et al., 2014). Reptiles and reptile-like vertebrates were ancestors of mammals and archosaurs (Laurin and Reisz, 1995). Non-crocodylian reptiles have intermediate degrees of ventricular septation (Jensen et al., 2014).

The single cardiac ventricle of extant non-crocodylian reptiles is partially divided by three septa named the 'vertical septum', the 'muscular ridge' and the 'bulbuslamelle'. The vertical septum is a prominent sheet of trabecular myocardium positioned beneath the atrioventricular valve (Fig. 1). It separates the oxygen-rich blood from oxygen-poor blood coming from the right atrium, its function resembling that of the ventricular septum of mammals and archosaurs (Jensen et al., 2014). The muscular ridge is the most prominent septal structure, but is not involved in the separation of the inflowing blood from the atria because it is positioned to the right of the atrioventricular canal (Poelmann et al., 2014, 2017) (Fig. 1), in contrast to the ventricular septum of mammals and archosaurs, which is positioned immediately below the atrioventricular canal (Cook et al., 2017; Greil, 1903; Webb et al., 1971). During ejection, the muscular ridge, however, forms an important boundary between the pulmonary compartment, the cavum pulmonale, and the cavum venosum to separate blood flow into the aortae and the pulmonary artery, respectively (Fig. 1). The third septum, the 'bulbuslamelle', is positioned opposite to the muscular ridge and presses against the free edge of the muscular ridge during contraction. It has been shown experimentally that this 'coming-together' of the two septa limits mixing of oxygen-rich blood and oxygen-poor blood during cardiac contraction (White, 1959). The full ventricular septum of mammals, birds and crocodylians has a pronounced left-right gradient of expression of the transcription factor *Tbx5* (Jensen et al. 2018; Koshiba-Takeuchi et al., 2009; Poelmann et al., 2014). Analyses of *Tbx5* gradients suggested that the vertical septum of a turtle (*Trachemys*), but not the vertical septum of a lizard (*Anolis*), is homologous to the full ventricular septum (Koshiba-Takeuchi et al., 2009). Studies on other species of turtles and squamate reptiles, however, show that both the muscular ridge and the vertical septum display a gradient of *Tbx5* expression (Poelmann et al., 2014). These seemingly conflicting results in non-crocodylian reptiles could be resolved when the expression of *Tbx5* would identify more than one septal structure in animals without a full ventricular septum.

Because the cardiac anatomy of the last common ancestor of amniotes is likely to remain unknown, we can only provide insight into the evolution of the ventricular septum through studies of the cardiac anatomy of extant reptiles. Among these, the monitor lizards (Varanidae) have ventricular septa that are more developed than in any other lizard (Brücke, 1852; Jensen, 2019; Webb et al., 1971). Further, monitors are exceptional among lizards because their cardiac ventricle is functionally divided, such that the left side of the ventricle (cavum arteriosum and venosum) generates high systemic blood pressures and the cavum pulmonale supplies the lungs at much lower pressures (Burggren and Johansen, 1982; White, 1968). Consequently, shunting of blood streams in the monitor ventricle is

[1]University of Amsterdam, Amsterdam UMC, Department of Medical Biology, Amsterdam Cardiovascular Sciences, Meibergdreef 15, 1105AZ, Amsterdam, The Netherlands. [2]Department of Developmental Cardiology, Institute of Physiology, Academy of Sciences of the Czech Republic, Vídeňská 1083, 142 20, Prague, Czech Republic. [3]Charles University, First Faculty of Medicine, Institute of Anatomy, U Nemocnice 3, 128 00, Prague, Czech Republic. [4]Department of Cardiology, Institute of Clinical Medicine, Aarhus University Hospital, Skejby, 8200, Aarhus, Denmark. [5]Department of Bioscience, Zoophysiology, Aarhus University, 8000, Aarhus, Denmark. [6]Department of Radiology and Nuclear Medicine, University of Amsterdam, Amsterdam UMC, Meibergdreef 9, 1105AZ, Amsterdam, The Netherlands.
*These authors contributed equally to this work

‡Authors for correspondence (david.sedmera@lf1.cuni.cz; b.jensen@amc.uva.nl)

D.S., 0000-0002-6828-3671; B.J., 0000-0002-7750-8035

Received 1 March 2019; Accepted 25 June 2019

Development (2019) 146, dev177121. doi:10.1242/dev.177121

almost independent of atrial filling pressures and the (arterial) afterloads, whereas in species without a functionally divided ventricle, atrial filling pressures and afterloads directly affect the shunting of blood streams in the ventricle (Hicks, 1998; Joyce et al., 2016). There are, nonetheless, minor degrees of so-called 'washout shunting' in the monitors (and other non-crocodylian reptiles) because the cavum venosum is a conduit for oxygen-poor blood in diastole and a conduit for oxygen-rich blood in systole (Heisler and Glass, 1985; Heisler et al., 1983; Ishimatsu et al., 1988). The mammal-like blood pressures and low levels of shunting in monitors support their metabolic rates, which are higher than in other reptiles (Thompson and Withers, 1997). The greater state of development of the septa could associate with more pronounced patterns of gene expression, in which case the monitor ventricle may be a very suitable model in which to test the evolutionary origin of the full ventricular septum.

To investigate whether the ventricle of monitors is divided by structures that are homologous to the full ventricular septum of mammals and archosaurs, we studied heart development and function in monitors (*Varanus acanthurus*, *V. exanthematicus*, *V. indicus* and *V. salvator*) and compared them with phylogenetically distant lizards with typical lizard hearts, the brown anole (*Norops sagrei*) and the leopard gecko (*Eublepharis macularius*). To assess homology between amniote cardiac structures, we studied the expression of anole orthologues of genes associated with the formation of the ventricular septum of mammals and birds, specifically *Irx1*, *Irx2*, *Tbx3*, *Tbx5* and *Myh6* (Aanhaanen et al., 2010; Boukens and Christoffels, 2012; Bruneau et al., 1999; Christoffels et al., 2000b; de Groot et al., 1987; Hoogaars et al., 2004; Moorman et al., 1998; Yamada et al., 2000). We then related the degree of septation to electrical function. In mammals, the activating current spreads from the atrioventricular node through the atrioventricular bundle that resides in the crest of the ventricular septum (Durrer et al., 1970; van Rijen et al., 2001). This mode of activation reveals itself on the epicardial surface as an early activation near the ventricular apex (Chuck et al., 2004; Reckova et al., 2003; Rentschler et al., 2001; Sankova et al., 2012). Electrical activation is much the same in crocodylians, which have a full ventricular septum, whereas activation of the undivided ventricle in lizards and snakes proceeds in a primitive pattern from base to apex (Christian and Grigg, 1999; Gregorovicova et al., 2018; Jensen et al., 2018, 2012). We hypothesize that the advanced state of ventricular septation in monitor lizards could impact on electrical propagation.

We show in monitors that the ventricular septa express orthologues of genes associated with the formation of the ventricular septum of mammals and birds and that the pattern of electrical activation is specialized compared with other squamate reptiles. The ventricle of monitors appears to be an extreme variation of the common design of the non-crocodylian reptilian ventricle.

RESULTS

The adult heart of monitors has a left and a right ventricle

The monitor ventricle consists mostly of trabeculated myocardium, as is the case in other squamates (Fig. 1). In the adult monitor ventricle (*V. exanthematicus* and *V. salvator*), the trabeculations are organized into a thick-walled and left-sided systemic 'left ventricle' and a thin-walled and right-sided pulmonary 'right ventricle', or cavum pulmonale (Fig. 2A,A′, Movie 1). The 'left ventricle' corresponds to the so-called cavum arteriosum and cavum venosum (Fig. 1, CA and CV, respectively). In the transverse plane, the 'left ventricle' is circular and the 'right ventricle' forms a crescent at its right side (Fig. 2B,B′, Movie 2). The two ventricles are separated by the muscular ridge and the bulbuslamelle (Fig. 2B). In the apical half of the ventricle, the two septa are fused and appear as one septum. We noticed highly echogenic lamellae in the inner-most part of the cavum venosum. These lamellae correspond to the so-called bulboauricular lamellae of Greil (Greil, 1903; Jensen et al., 2013). In a large heart of *Varanus salvator*, these lamellae were thick and constituted the inner-most part of the muscular ridge and bulbuslamelle (Fig. 2C). They extended from the atrioventricular canal to the point where the muscular ridge and bulbuslamelle abut during contraction.

In diastole, the atrioventricular valve achieved direct contact with a prominent vertical septum (Fig. 2D, Movie 3). The vertical septum was positioned entirely within the cavity of the left ventricle (the cavum arteriosum and cavum venosum combined). Both atrial blood flows were therefore received in the left ventricle. As atrial blood enters the ventricle, the space between the muscular ridge and the bulbuslamelle widens, allowing the right atrial blood to reach the cavum pulmonale (the right ventricle). In systole, this space closes again as the muscular ridge and the bulbuslamelle abut. Then, the

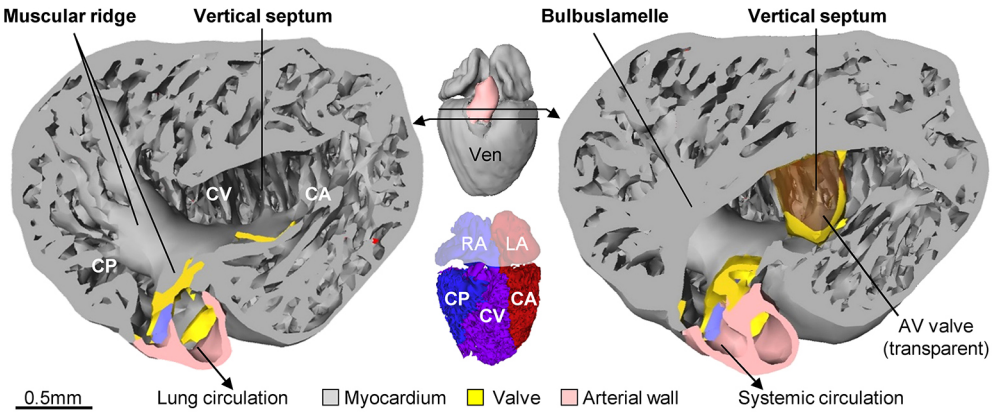

Fig. 1. Septa and sub-compartments in a typical lizard ventricle. The luminal side of the lizard ventricle, looking towards the ventricular apex, shown from two transverse cuts made in the ventricular base. Images are taken from a 3D model of the heart of an adult anole lizard, from Jensen et al. (2014). There are three septa (muscular ridge, bulbuslamelle, vertical septum), none of which fully separates the ventricular cavity. Accordingly, the division into three sub-compartments is not based on strict boundaries, but inferred from anatomy and blood flow (Jensen et al., 2014): cavum arteriosum (CA, red in inset), cavum venosum (CV, purple in inset) and cavum pulmonale (CP, blue in inset). Notice the vertical septum is beneath the atrioventricular valve (AV valve, made transparent). LA, left atrium; RA, right atrium; Ven, ventricle.

Development (2019) 146, dev177121. doi:10.1242/dev.177121

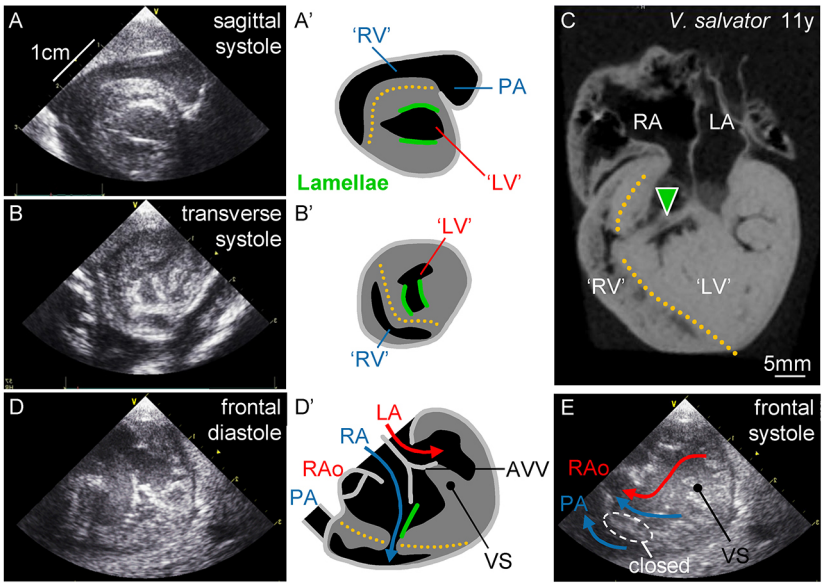

Fig. 2. The monitor ventricle is divided. (A,A′) Echocardiography of the ventricle and schematic of the savannah monitor showing a densely muscular left ventricle ('LV') and a less muscular right ventricle ('RV') leading to the pulmonary artery (PA). The echogenic lamellae (green) are the bulboauricular lamellae of Greil (Greil, 1903). They constitute the inner-most part of the muscular ridge and bulbuslamelle. (B,B′) In the transverse plane, the right ventricle forms a semi-circle as it does in mammals and birds, nestled against the contracting muscular ridge and bulbuslamelle (orange dotted line). (C) The contracted ventricle of the water monitor (visualized with MRI) is similar to the ventricle of the savannah monitor and shows a pronounced bulboauricular lamella (green arrowhead). (D-E) In ventricular diastole of the savannah monitor (D), the atrioventricular valve (AVV) contacts the vertical septum (VS) and the blood streams of the left atrium (LA) and right atrium (RA) are separated along it, as the atrial blood streams are along the ventricular septum of mammals and archosaurs. To reach the right ventricle, blood from the right atrium has to pass through the left ventricle and the small gap between the muscular ridge and bulbuslamelle (D′, blue arrow). In systole (E), contractions close the gap ('closed') and the muscular ridge and bulbuslamelle now separate the low-pressure right ventricle from high-pressure left ventricle, as does the ventricular septum of mammals and archosaurs (D and E are screenshots of a previously published movie; Jensen et al., 2014). Red arrows indicate the direction of flow of oxygen-rich blood. Blue arrows indicate the direction of flow of oxygen-poor blood. RAo, right aorta.

'right ventricle' ejects into the pulmonary trunk and the 'left ventricle' ejects into the aorta (Fig. 2E, Movie 3). Septal structures of the monitor ventricle show functional and anatomical resemblance to the ventricular structures of four-chambered hearts of mammals and archosaurs. Next, we wanted to know whether the septal structures of monitors develop in a similar fashion to the four-chambered heart.

Features of monitor heart development that are shared with other squamates

We examined the development of the morphology of the monitor heart in a series of sections of mangrove monitor hearts stained for a marker for cardiac muscle (cardiac troponin I). In the earliest specimen, from 10 days post-oviposition (dpo), the heart was similar to that of other reptiles and to chicken around 4 days of development; that is, myocardium was detected in the sinus venosus, sinuatrial junction, atria, atrioventricular canal, ventricle, and outflow tract (Fig. S1A,B). The ventricle was proportionally small, whereas the atrioventricular canal and myocardial outflow tract, the conus arteriosus, were proportionally large, indicating that the heart was immature (Figs S1,S2). In the atria, formation of trabeculae was just beginning and the atrial septum was a low myocardial ridge with a mesenchymal cap in the atrial roof (Fig. S1C). A non-muscular dorsal mesenchymal protrusion was present in the dorsal wall of the atrium. The atrioventricular canal was circular in cross-section and its interior was occupied by the large dorsal and ventral cushions (Fig. S1D). It was positioned to the immediate left of the body midline as defined by the position of the notochord, foregut and trachea (Fig. S1A). Trabeculation of the ventricle was prominent in the outer curvature and absent in the inner curvature (Fig. S1A). Distally, the trabeculated muscle was sponge-like, whereas proximally it was organized into about 12 sheets of trabecular muscle that were oriented approximately dorso-ventrally (Fig. S1A). The outflow tract was proportionally long, it was myocardial to the vicinity of the pericardial reflection, and its interior was dominated by mesenchyme but the lumen was not divided (Fig. S1A,B).

In the next stage investigated, 24 dpo (Fig. 3A), all three sinus horns were distinct vessels and their myocardium extended to the pericardial reflection (Fig. S1E,F). The atrial septum was developed to such an extent that the ostium primum was almost closed and secondary foramina had formed (Fig. S1F,G). Myocardium was detected within the dorsal mesenchymal protrusion (Fig. S1E). The atrioventricular canal remained positioned to the left of the body midline, but its cushions had begun to merge. The formation of the muscular ridge had begun near the base of the outflow tract, but the outer curvature of the ventricle comprised trabecular myocardium only (Fig. 3A, Fig. S1F). A shallow sulcus was found on the epicardial surface in proximity of the early muscular ridge (Fig. 3A, Fig. S1E-G). The outflow tract was myocardial only in the proximal half (Fig. S1G). Its lumen was divided by mesenchyme into three channels, the future pulmonary artery, the left aorta and the right aorta. At this stage, the proportions of the principal compartments of the heart had become similar to those of the formed heart. Nevertheless, the size of the ventricle still had to increase at the expense of the myocardial outflow, by regression of the myocardial outflow tract (Fig. S2). Furthermore, ventricular septation was not obviously different from that of other lizards.

Development (2019) 146, dev177121. doi:10.1242/dev.177121

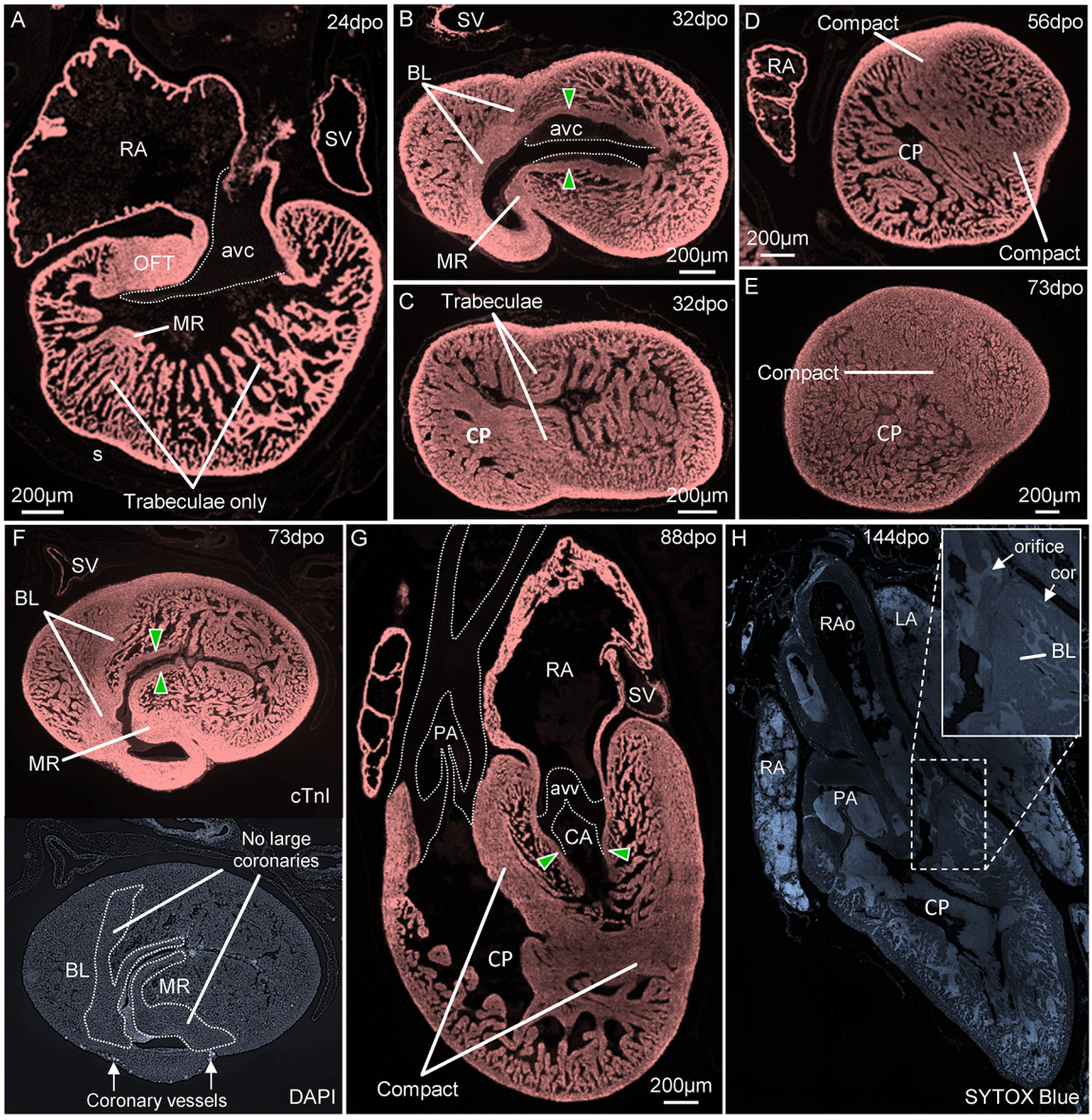

Fig. 3. Morphogenesis of the mangrove monitor heart. (A) Frontal section of the heart of a 24 dpo specimen, showing that ventricular trabeculae are extensive. Septation (formation of the muscular ridge) is subtle but appears as densely organized myocardium and appears to associate with a shallow ventricular sulcus (s). (B,C) At 32 dpo, the muscular ridge and the bulbuslamelle are recognizable by compact myocardium. The bulboauricular lamellae (green arrowheads) are much developed. However, at mid-height of the ventricle (C), the compact myocardium of the muscular ridge and the bulbuslamelle blends into trabeculae. (D,E) At 56 dpo, some ventricular trabeculae of the apical region show a more compact organization and at 73 dpo the apex is divided by a compact septum. (F) In the ventricular base at 73 dpo, the muscular ridge and bulbuslamelle have a core of compact muscle, but coronary vessels appear to be confined to the sub-epicardial layers. (G) At 88 dpo, compact myocardium fully separates the cavum arteriosum from the cavum pulmonale. The bulboauricular lamellae (green arrowheads) extend deep into the cavum arteriosum. (H) At 144 dpo, coronary arteries can be found in the outer compact wall of the ventricle, but comparable vessels were not found in the septal structures. avc, atrioventricular cushion; avv, atrioventricular valve; BL, bulbuslamelle; CA, cavum arteriosum; cor, coronary vessel; CP, cavum pulmonale; LA, left atrium; MR, muscular ridge; OFT, outflow tract; PA, pulmonary artery; RA, right atrium; RAo, right aorta; SV, sinus venosus.

Specialized anatomical features of monitor ventricular septation

By 32 dpo, the ostium primum was closed and specialized features had started to become apparent. By 32 dpo, the muscular ridge and the bulbuslamelle were characterized by a core of compact myocardium (Fig. 3B). Towards the apex, the compact myocardium dissolved into trabeculae (Fig. 3C). The trabecular sheets beneath the atrioventricular cushions were of approximately equal height. There was no obvious vertical septum at this stage. The bulboauricular lamellae were becoming prominent (Fig. 3B). In the next stages investigated, 56 and 73 dpo, parts of the apical trabeculae appeared to be organized in a more compact fashion (Fig. 3D,E). The vertical septum started to appear as a prominent sheet of trabeculae beneath the atrioventricular valves. Subepicardial coronaries were detected by 73 dpo, by a high density of DAPI (the erythrocytes are nucleated and DAPI positive), but the septal components appeared without coronary vasculature (Fig. 3F). At 88 and 144 dpo, compact muscle enclosed the cavum arteriosum and venosum and thus separated these parts from the cavum pulmonale, except at the gap between the muscular ridge and the bulbuslamelle (Fig. 3G,H). The bulboauricular lamellae were prominent (Fig. 3G). The atrioventricular canal remained positioned to the left of the aortic

Development (2019) 146, dev177121. doi:10.1242/dev.177121

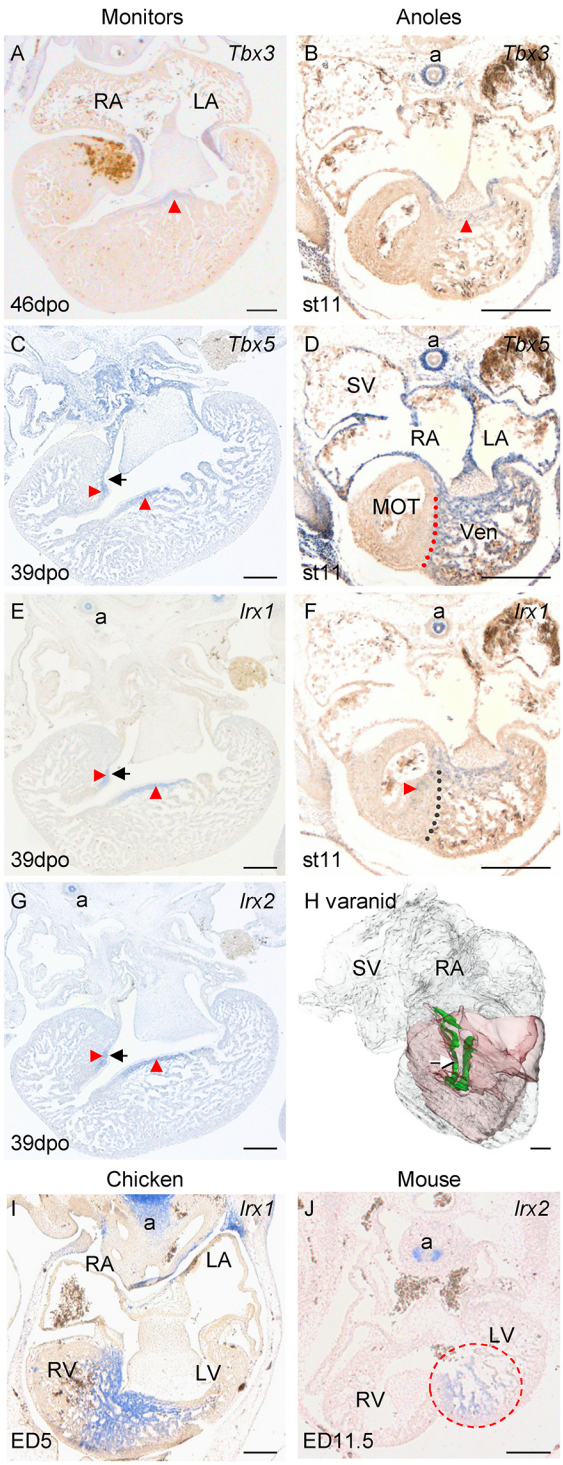

Fig. 4. Septal structures in monitors, anoles, chicken and mouse express homologous genes. (A,B) In monitors, *Tbx3* was expressed from the atrioventricular canal to the vicinity of the vertical septum (red arrowhead), much like in the anole, but more pronounced. (C) *Tbx5* was expressed throughout the monitor ventricle and was particularly rich in the bulboauricular lamellae and the connected crests of trabecular sheets (red arrowheads). The black arrow points to the outflow tract cushion on the bulbuslamelle. (D) In the brown anole, *Tbx5* was uniform in the ventricle, but absent from the myocardial outflow tract (MOT). (E-G) In monitors, the bulboauricular lamellae and the connected crests of trabecular sheets expressed *Irx1* and *Irx2* (red arrowheads), and in the brown anole (F), *Irx1* was expressed like in the monitors and extended beyond the *Tbx5* gradient (dotted line) to the muscular ridge. (H) The myocardium of a 56 dpo mangrove monitor seen from the right was rich in *Tbx3*, *Tbx5*, *Irx1* and *Irx2* (green), together with the totality of the muscular ridge and bulbuslamelle (transparent red) in a reconstruction of all myocardium (transparent grey). The white arrow indicates the gap between the muscular ridge and bulbuslamelle. (I) Ventricular expression of *Irx1* in the forming septum of chicken. (J) Ventricular expression of *Irx2* in the forming septum of mouse (encircled). Notice that transcripts were detected in the developing airways. a, airway; ED, embryonic day; LA, left atrium; LV, left ventricle; RA, right atrium; RV, right ventricle; st, Sanger stage; SV sinus venosus; Ven, ventricle.

base. At these late gestational stages, the lumen of the cavum pulmonale was approximately 50% of the total ventricular lumen, but this proportion was less than 30% in two juvenile specimens (Fig. S2). In the 144 dpo specimen, a coronary artery with an approximately 50 µm diameter orifice had its origin in the sinus of the dorsal leaflet of the right aorta. Although we could detect coronary vessels in the outer compact walls, comparable vessels were not found in the compact muscle of the septa (Fig. 3H). In the hearts of two juveniles and two adult savannah monitors, the muscular ridge, the bulbuslamelle and the outer compact wall did contain coronary vessels (Fig. S3).

Septation of the monitor ventricle appears to involve compaction of trabeculae, much like it does in chicken. Therefore, we hypothesized that the monitor septa would express genes associated with the development of the full ventricular septum.

Monitor septal structures express orthologues of transcription factors of the full ventricular septum

For *in situ* hybridization analysis of embryonic lizards, we compared monitors with *Norops sagrei*, which has a typical lizard heart. We focused on the stages when septal structures have formed and when the ventricle has grown to the extent that its proportion of the total cardiac mass is almost the same as that of adult animals, i.e. ∼70-80% (Fig. S2); in *Varanus acanthurus* this corresponded to ∼35 dpo and in *Norops sagrei* to Sanger stage 11 (Jensen et al., 2013; Sanger et al., 2008). In the monitors, *Tbx3* was expressed in the bulboauricular lamellae from the atrioventricular canal to the vicinity of the vertical septum (Fig. 4A). This expression domain, along with the bulboauricular lamellae, extended deeper into the ventricle than it did in *Norops* (Fig. 4A,B). In the monitors, *Tbx5* was expressed throughout the ventricle, with no gradient between the left and right sides (Fig. 4C). The myocardial outflow tract did not express *Tbx5*. Within the ventricle, *Tbx5* was particularly rich in the bulboauricular lamellae and therefore enriched near the vertical septum and in the inner-most parts of the muscular ridge and the bulbuslamelle (Fig. 4C). In *Norops*, the bulboauricular lamellae were less developed and they were not enriched in *Tbx5* expression (Fig. 4D). In the monitors, *Irx1* and *Irx2* were expressed in the bulboauricular lamellae and therefore near the vertical septum and in the inner-most parts of the muscular ridge and the bulbuslamelle (Fig. 4E,G). *Irx1* and *Irx2* were similarly expressed in the ventricles of the monitors and *Norops*, although the patterns were more pronounced in the monitors (Fig. 4E-G). Fig. 4H shows a 3D reconstruction of the myocardium in the *Varanus indicus* ventricle (56 dpo), which expressed *Irx1*, *Irx2* and *Tbx5*. In the monitors, the inner-most parts of the muscular ridge and the bulbuslamelle associated with one large cushion each (Fig. 4C,E,G, black arrows), which persisted after hatching (Fig. S4). Similar cushions are found in other squamates with ventricles with pressure separation (Jensen et al., 2014; Jensen et al., 2010). In *Norops*, *Irx1* expression extended beyond the domain of *Tbx5* expression and into the outflow tract myocardium (Fig. 4F, Fig. S5). Fig. 4I and 4J show

Development (2019) 146, dev177121. doi:10.1242/dev.177121

Irx1 and *Irx2* expression in the septal region of chicken and mouse, respectively. Outside the heart, *Tbx3*, *Tbx5*, *Irx1* and *Irx2* were also detected in the developing trachea and bronchi (Fig. 4), and *Irx1* and *Irx2* in the spinal cord, homologous to the expression patterns observed in mouse and chicken (Chapman et al., 1996; Christoffels et al., 2000b; Gibson-Brown et al., 1998).

We have previously shown specific detection of *Myh6* expression in the atrioventricular junction of the American alligator, using a *Norops Myh6* probe (Jensen et al., 2018). In embryonic mammals and chicken, *Myh6* is initially expressed in the ventricle but becomes confined to the forming atrioventricular bundle (de Groot et al., 1987; Moorman et al., 1998; Yutzey et al., 1994). We investigated whether transcripts of *Myh6* associated with particularly developed bulboauricular lamellae. Across a phylogenetic diverse set of non-crocodylian reptiles, *Myh6* was detected in the atria and atrioventricular canal of all species (Fig. 5). Only in monitor lizards, however, did we observe *Myh6* expression in the bulboauricular lamellae in the ventricle (Fig. 5). In the leopard geckos, *Myh6* was expressed in a pattern similar to that observed in *Norops*, i.e. readily detected in the atria (and sinus venosus), but not in the ventricle (Fig. 5). Fig. 5 shows sections of both adult and developing hearts. We then compared multiple stages of developing *Norops* and monitors, but only in the monitors did we detect prominent expression in the bulboauricular lamellae (Fig. S6).

Taken together, the expression of genes associated with the ventricular septum of mammals and birds was found around the ventricular septal structures of monitors. The myocardium immediately adjacent to the vertical septum of the monitors had a molecular phenotype comparable to that of the atrioventricular bundle of mammals and birds, which led us to hypothesize that this myocardium would be activated early, as it is in mammals and birds.

Early activation of the ventricular myocardium in the vicinity of the vertical septum in monitors

Optical mapping of cardiac action potentials was performed on six ridge-tailed monitor embryos ranging from 21 to 46 dpo, spanning the period when ventricular septa are formed. Despite substantial growth of the embryo and heart during this period, the intrinsic heart rate, atrial activation time, atrioventricular delay and ventricular activation times remained essentially constant (Fig. S7). The left side of the ventricle was consistently activated earlier than the right side (Fig. 6A,C). On the left side, the earliest epicardial activation was always observed in the vicinity of the forming vertical septum. In the oldest embryos, this was seen as a site of activation relatively deep in the ventricle (Fig. 6C), which was different from the primitive base-to-apex activation of the leopard geckos (n=11; Fig. 6B). This pattern of activation could be elicited by stimulation in the apical region of the left chamber (only performed in the oldest and largest specimens; data not shown).

DISCUSSION

Monitor lizards are the only lizards we know of with a divided ventricle. Here, we establish that the dividing septa express *Irx1*, *Irx2*, *Tbx3* and *Tbx5*. In all studied ventricles with haemodynamically distinct left and right sides, i.e. human, mouse, chicken and crocodylians, these transcription factors are expressed in the septal structures and deficiency of *Tbx3* and *Tbx5* are known to cause ventricular septal defects (Bakker et al., 2008; Bruneau et al., 1999, 2001; Christoffels et al., 2000b; Hoogaars et al., 2004; Jensen et al., 2018; Sizarov et al., 2011; Yamada et al., 2000). In mammals, chicken and crocodilians, *Tbx3* delineates the atrioventricular conduction axis (Jensen et al., 2018) and the deeper ventricular

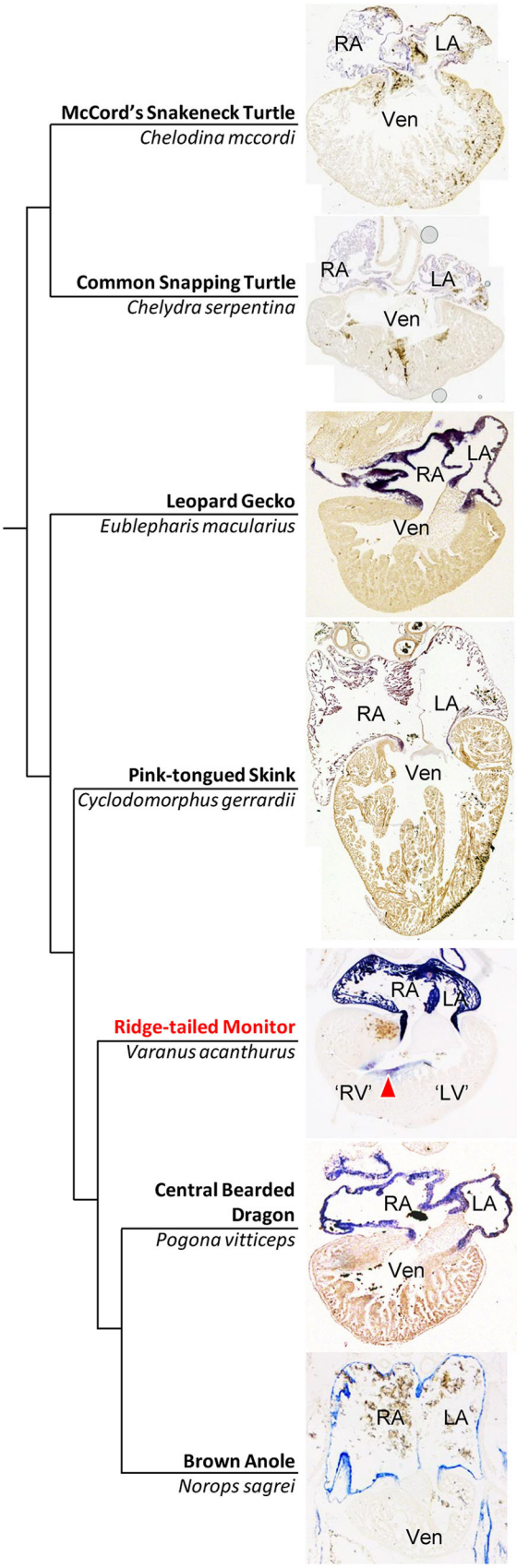

Fig. 5. Cardiac expression of *Anolis* atrial myosin heavy chain (*Myh6*) identifies the bulboauricular lamellae in monitors only (red arrowhead). LA, left atrium; 'LV', monitor left ventricle; RA, right atrium; 'RV', monitor right ventricle; Ven, single ventricle.

Development (2019) 146, dev177121. doi:10.1242/dev.177121

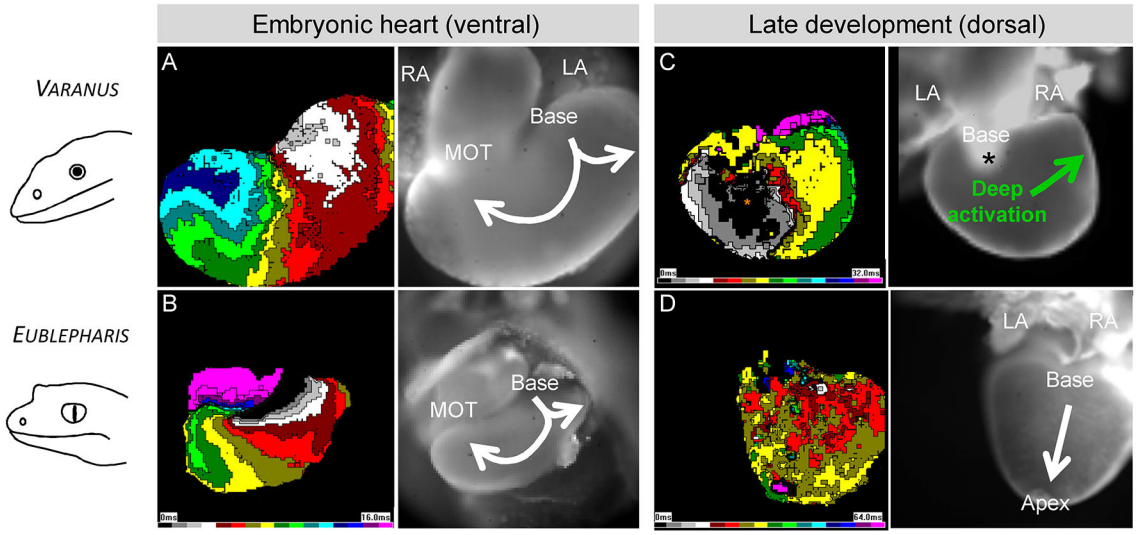

Fig. 6. Ventricular activation becomes specialized in monitors. (A,B) In the embryonic hearts of both the ridge-tailed monitor (21 dpo) and the leopard gecko (7 dpo), ventricular activation initiated in the base and swept over the apex and towards the myocardial outflow tract (MOT). The time of activation is color-coded such that shades of gray are early and purple is late. This time scale is 16 ms for A and B, 32 ms for C and 64 ms for D. The arrows indicate the direction of the activation front. (C) In later development of the monitors (46 dpo shown), early activation was deep (black field) towards the apex on the left and therefore specialized. The black asterisk indicates the approximate position of the crest of the vertical septum. (D) In later development of the leopard gecko (53 dpo), early activation was in the ventricular base, and total activation exhibited the primitive base-to-apex pattern. LA, left atrium; RA, right atrium.

expression of *Tbx3* in the monitors was associated with a deeper initial electrical activation. Only in the monitors did the expression of these transcription factors colocalize with the expression of *Myh6*, which resembles the setting in four-chambered hearts, whereas *Myh6* was not found in the ventricles of the six non-varanid species we investigated. Therefore, we consider it likely that conserved molecular mechanisms underlie the processes of ventricular septation in all known instances. Our results suggest that the various degrees of septation encountered in Sauropsida (reptiles and birds) and Synapsida (mammals) are variations of the same building plan inherited from their common amniote ancestor. Incidentally, we found the same transcription factors to be expressed in the trachea and bronchi, as have been observed in the developing trachea and bronchi of mouse and chicken (Chapman et al., 1996; Christoffels et al., 2000b; Gibson-Brown et al., 1998). Therefore, homologous molecular mechanisms also appear to drive the formation of the main airways despite the considerable anatomical differences in the formed respiratory systems of reptiles and mammals (Farmer and Sanders, 2010; Perry and Sander, 2004; Schachner et al., 2014).

The muscular ridge and the bulbuslamelle could both be identified by the compact organization of their myocardium. In the early stages, this myocardium blended into apical trabeculae, whereas at later stages the compact muscle of the muscular ridge and the bulbuslamelle could be followed to the apex. This strongly suggests that some trabeculae had undergone compaction, seemingly in the absence of coronary vasculature. Compaction is considered a key process of the formation of the ventricular walls and septum of mammals and birds (Captur et al., 2015; Sedmera et al., 2000), although the importance of the process may vary between species and its contribution to pathology has been debated (Anderson et al., 2017; Finsterer et al., 2017). Whereas the process of compaction is generally thought to be the coming-together of trabeculae (Anderson et al., 2017; Finsterer et al., 2017), foundational observations made in chicken suggested that compaction is the thickening of trabeculae to the extent to which the inter-trabecular spaces become obliterated (Rychterova, 1971). The trabeculae near the ventricular septa of the developing monitors had a dense organization as if the trabeculae were coming together (Fig. S1E-G), but they also appeared to be thicker like the trabeculae in the cavum pulmonale (Fig. 3D). It is possible that both processes of coming-together and thickening of the trabeculae contribute to compaction in monitors.

The muscular part of the human ventricular septum has been described by anatomists as having distinct components, specifically an inlet part (dorsal/posterior and a-trabecular), an apical part (surrounded by trabeculae), and an outlet part (ventral/anterior and without trabeculae) (Anderson and Becker, 1980; Van Mierop and Kutsche, 1985; Wenink, 1981). Molecular markers that distinguish these components remain to be found. Comparative anatomical studies concluded that the outlet part corresponds to the muscular ridge (Benninghoff, 1933; Poelmann et al., 2014; Van Mierop and Kutsche, 1985; Webb, 1979). Indeed, the muscular ridge of non-crocodylian reptiles expresses *Tbx5* in a gradient, as does the ventricular septum of mammals, chicken and crocodylians (Jensen et al., 2018; Koshiba-Takeuchi et al., 2009; Poelmann et al., 2014). Because the muscular ridge is not positioned beneath the atrioventricular junction it cannot be equated wholesale to the muscular part of the full ventricular septum (Benninghoff, 1933; Poelmann et al., 2014; Van Mierop and Kutsche, 1985; Webb, 1979). A gradient of *Tbx5* is also present on the ventral-most part of the bulbuslamelle. However, in mammals and birds this part seems to contribute to the right atrioventricular valve rather than the septum (Jensen and Moorman, 2016; Jensen et al., 2013; Lamers et al., 1995). The dorsal-most part of the bulbuslamelle is thought to contribute to the ventricular septum (Benninghoff, 1933; Greil, 1903; Jensen et al., 2014; Webb, 1979), but this part was not enriched for any of the investigated transcripts and did not have a gradient of *Tbx5*. Therefore, when comparing the muscular ridge and the bulbuslamelle of monitors with the ventricular septum of mammals and birds, there is a shared expression of key transcription factors but a divergence in the anatomy of the myocardial tissues that express these genes. In reptiles, the vertical septum is beneath the atrioventricular junction and the adjacent myocardium was enriched in transcripts associated with the atrioventricular bundle of mammals and archosaurs (Bakker et al., 2008; Jensen et al., 2018).

Development (2019) 146, dev177121. doi:10.1242/dev.177121

The early electrical activation near the vertical septum corroborates this interpretation. The final component of the full ventricular septum is the membranous septum (Cook et al., 2017; Greil, 1903; Jensen et al., 2014; Webb, 1979). The membranous septum develops from mesenchyme of the atrioventricular cushions and of the proximal part of the two mesenchymal ridges of the myocardial outflow tract (Anderson et al., 2014, 2019; Asami, 1969). Two similar mesenchymal ridges can be found in the developing outflow tract of reptiles, which apparently persist in monitors and pythons as large cushions of connective tissue at the point where their muscular ridge and bulbuslamelle abut (Greil, 1903; Jensen et al., 2014, 2010; Poelmann et al., 2017). If, in a reptile setting, these cushions were to fuse, not only would the ventricle be fully divided, but the membranous septum would also be closely aligned with the arterial wall that separates the pulmonary artery from the aorta (Fig. S4C).

If the cushions of the muscular ridge and the bulbuslamelle fused, the right atrial blood would only fill the cavum venosum and would not be able to reach the cavum pulmonale behind this hypothetical membranous septum. Interestingly, in developing mammals and archosaurs, the atrioventricular canal undergoes a pronounced rightward expansion during the process of ventricular septation whereby the right atrium remains in contact with the right ventricle (Jensen and Moorman, 2016; Jensen et al. 2013; Lamers et al., 1995). This process includes the formation of the right atrioventricular valve. Failed expansion results in congenital malformations, such as tricuspid atresia and double inlet left ventricle, which have been reported in multiple mammalian species (Jensen and Moorman, 2016; Michaëlsson and Ho, 2000). In squamate reptiles with an undivided ventricle, the atrioventricular canal is positioned to the left of the body midline (Jensen et al., 2013) and does not undergo a rightward expansion (Jensen and Moorman, 2016). That the atrioventricular canal of monitors remains left-sided, shows that the right-wards remodelling of the atrioventricular canal associates with full ventricular septation only. Consequently, the cavum venosum of monitors serves as the conduit for systemic venous blood to the cavum pulmonale in ventricular diastole and serves as the conduit for pulmonary venous blood in systole as it does in other squamates (Fig. 2D-E). So-called washout shunting is therefore inherent to the monitor heart (Heisler and Glass, 1985). The wash-out of systemic venous blood to the systemic arterial circulation, or so-called right-to-left shunting, is greater than left-to-right shunting in monitors (Heisler and Glass, 1985; Heisler et al., 1983; Ishimatsu et al., 1988), consistent with our finding that the cavum pulmonale is smaller than the cavum venosum and cavum arteriosum.

Anatomists and physiologists have long emphasized that the heart of monitors can be seen as a conceptual stage between the hearts of non-crocodylian reptiles and the fully septated hearts of crocodylians, birds and mammals (Acolat, 1943; Brücke, 1852; Greil, 1903; Jensen et al., 2014). The primitive (left-sided) position of the atrioventricular canal concomitant with the specialized state of deep left ventricular activation corroborates this notion. Comparing lizards, crocodylians, birds and mammals, we find considerable overlap in the functional anatomy, electrophysiology, and molecular phenotype of the septation of the ventricles of amniotes. Our results suggest that Sauropsida and Synapsida inherited precursor structures from their common amniote ancestor. Particular features evolved within each lineage (Cook et al., 2017), but we propose that they could be seen as variations on a common design. In the special case of monitor lizards, we suggest that ventricular septation relies on evolutionarily conserved building blocks and results in a convergence of function despite a divergence of appearance.

MATERIALS AND METHODS

Animals

Of the savannah monitor (*Varanus exanthematicus*, Bosc 1792), we used one adult for echocardiography (body mass ∼2 kg), hearts of two adults (unknown body mass) and two juveniles (body mass 18 and 22 g) for histology stained with Picro-Sirius Red. We used the heart of one 11-year-old water monitor (*V. salvator*, 10 kg), visualized with MRI, that was donated to us (B.J.) after the animal died from senescence. From six fertilized eggs of ridge-tailed monitor (*Varanus acanthurus*, Boulenger 1885) that were incubated at 30°C and 80-90% humidity, we investigated hearts isolated on the following dpo: 15, 21, 25, 32, 39 and 46. From 11 fertilized eggs of leopard gecko (*Eublepharis macularius*, Blyth 1854) that were incubated similarly, hearts were isolated on the following days: 7, 11, 15 (n=2), 18, 26 (n=2), 32, 40, 47 and 53. We further made use of a previously published developmental series of the mangrove monitor (*Varanus indicus*, Daudin 1802) (Gregorovicova et al., 2012). The hearts of this series were used for immunohistochemistry of heart muscle only, as initial tests showed that the tissue preservation was not good enough for the detection of most antigens and gene transcripts by *in situ* hybridization. Of the brown anole (*Norops sagrei*, Duméril and Bibron 1837), we investigated embryos of Sanger stages (Sanger, Losos, and Gibson-Brown, 2008) 7 (n=1), 9 (n=1), 11 (n=2), 16 (n=1), and one adult, approximately 1 year old. The handling of the adult brown anole complied with Dutch national and institutional guidelines (Amsterdam UMC, The Netherlands) and with the Institutional Animal Care and Use Committee of the University ratified approval registered as 'DAE101617'. All data were generated within the time limits of DAE101617.

Echocardiography

One adult savannah monitor (*V. exanthematicus*) was anaesthetized with isoflurane and intubated for manual ventilation with room air containing 1.5% isoflurane. Images were obtained at room temperature while the lizard was placed on its back on a heating pad set at 25°C. We used a Vivid 7 echocardiographic system (GE Healthcare) with an 11 MHz phased array paediatric transducer operating at a frame rate of 60 Hz. Two-dimensional images were recorded in the three principal planes of the body (sagittal, transverse and frontal) and stored for off-line evaluation on a workstation (EchoPac Dimension 06, GE Healthcare).

Optical mapping

Optical mapping was performed on *V. acanthurus* and *Eublepharis macularius*. Shell and membranes were removed and the embryos were placed in a dish containing ice-cold reptilian Ringer solution (specific Ringer solutions for *Anolis* adopted from Jensen et al., 2012); in mmol/l: NaCl 95, Tris 5, NaH_2PO_4 1, KCl 2.5, $MgSO_4$ 1, $CaCl_2$ 1.5, glucose 5, pH adjusted to 7.5 with HCl). The heart and adjacent posterior body wall structures were isolated and stained in 2.5 mmol/l di-4-ANEPPS (Invitrogen) for 10 min. Contractions were inhibited with cytochalasin D (0.2 µM, Sigma) and the torso was pinned to the bottom of the dish containing oxygenated Ringer solution at 28°C. Imaging was performed from both the ventral and dorsal surfaces at 0.25-1 kHz. Ventricular pacing was performed in the three oldest specimens of both species using a platinum electrode at 125% of the intrinsic rate and twice the diastolic threshold (Sedmera et al., 2003). Data acquisition and analysis were performed using an Ultima L high-speed camera and bundled software (Sankova et al., 2012). Epicardial activation maps were then constructed separately for the ventral and dorsal (as well as lateral, when available) ventricular surfaces in sinus and stimulated rhythm.

Fixation, *in situ* hybridization and immunohistochemistry

For *V. acanthurus*, the hearts and surrounding tissues were fixed for 1 day in freshly made 4% paraformaldehyde in PBS (0.9% NaCl) and then washed twice in PBS before being stored in 70% ethanol. For *in situ* hybridization, we used previously published probes for *Anolis* mRNA (*Tbx3*, *Tbx5*, *Ttnnt2*, *Myh6*; Jensen et al., 2018; Jensen et al., 2012) and new probes based on the following coordinates using UCSC Genome Browser on Lizard May 2010 (Broad AnoCar2.0/anoCar2) Assembly; *Irx1* (chrUn_GL343292:777,311-778,155), *Irx2* (chrUn_GL343292:1,436,684-1,440,677). Tests with *Anolis*

Bmp2 and *Gja5* (Cx40) (also from Jensen et al., 2012) did not show specific stain in *Varanus*. *In situ* hybridizations were performed as described previously (Moorman et al., 2001) and performed on a series of sections of 8, 10 or 12 µm thickness that contained the entire heart of specimens of all *V. acanthurus*. The data displayed in Fig. 4I,J were generated in connection with the study by Christoffels et al. (2000a). For immunohistochemistry, sections of the embryonic hearts of *V. indicus* were cooked under pressure for 5 min in antigen retrieval solution (H-3300, Vector Laboratories). Myocardium was bound with a mouse polyclonal antibody to cardiac troponin I (Millipore, RRID: AB_11212281, 1:250). The antibody was detected with a fluorescently labelled secondary donkey-anti-mouse antibody (Invitrogen, RRID: AB_2556542, 1:200) conjugated to Alexa Fluor 488. Subsequently, sections were mounted using glycerol-PBS (1:1) containing SYTOX Blue (Invitrogen, S11348, 1:40.000) or DAPI (Sigma-Aldrich, D9542, 1:1000) for nuclear staining.

Magnetic resonance imaging (MRI)

For the MRI acquisition of the heart of the *V. salvator*, a 3.0T MR scanner (Ingenia; Philips Medical Systems, Best, The Netherlands) was used. For signal reception, a 32-channel head coil was used. For the 3D MRI acquisition, a T1 weighted turbo-field echo (TFE) pulse sequence was used with the following imaging parameters: TR/TE=6.7/2.9 ms, FA=20°, acquired voxel size=0.5×0.5×0.5 mm, NSA=2. Total scan duration was 7 min 23 s. The presented image is a thin MinIP (minimal intensity projection) magnetic resonance image reconstruction (5 mm slice thickness).

3D reconstructions

Reconstructions were made in Amira software (FEI) version 5.5 as described previously (Soufan et al., 2003). In the few cases in which a section was damaged (less than 10% of all images in a given preparation), its image was replaced by the nearest intact sister section. Images were aligned using the Align tool, including automatic alignment supplemented by manual fitting. Once aligned, signal was annotated using a manually set threshold. Surface files were made of label files that were resampled to a voxel size of approximately 10×10×10 µm.

Acknowledgements

We received valuable help from Corrie de Gier-de Vries with *in situ* hybridization and immunohistochemstry, and from Jaco Hagoort with Amira reconstructions.

Competing interests

The authors declare no competing or financial interests.

Author contributions

Conceptualization: A.F.M.M., T.W., V.M.C., D.S., B.J.; Methodology: J.H., J.M.N., R.N.P., D.S., B.J.; Formal analysis: J.H., M.G., V.M.C., D.S., B.J.; Investigation: J.H., M.G., J.M.N., R.N.P., D.S., B.J.; Writing - original draft: V.M.C., D.S., B.J.; Writing - review & editing: A.F.M.M., T.W., B.J.; Supervision: B.J.

Funding

This work was supported by Carlsbergfondet [CF14-0934 to B.J.], the Czech Ministry of Education [PROGRESS Q38 to D.S.], Akademie Věd České Republiky (Czech Academy of Sciences) [RVO: 67985823 to D.S.], Grantová Agentura České Republiky (Grant Agency of the Czech Republic) [16-02972S to D.S.], the Danish Natural Science Research Council [T.W.], and the Nederlandse Hartstichting COBRA3 [V.M.C.].

Supplementary information

Supplementary information available online at
http://dev.biologists.org/lookup/doi/10.1242/dev.177121.supplemental

References

Aanhaanen, W. T., Mommersteeg, M. T., Norden, J., Wakker, V., de Gier-de, V. C., Anderson, R. H., Kispert, A., Moorman, A. F. and Christoffels, V. M. (2010). Developmental origin, growth, and three-dimensional architecture of the atrioventricular conduction axis of the mouse heart. *Circ. Res.* **107**, 728-736. doi:10.1161/CIRCRESAHA.110.222992

Acolat, L. M. (1943). Contribution àl'anatomie comparée du cœur, et en particulier du ventricule, chez les batraciens et chez les reptiles. PhD thesis, Faculté des Sciences de Nancy, Besançon, France.

Anderson, R. H. and Becker, A. E. (1980). *Cardiac Anatomy: Integrated Text and Colour Atlas*. London: Churchill Livingstone.

Anderson, R. H., Spicer, D. E., Brown, N. A. and Mohun, T. J. (2014). The development of septation in the four-chambered heart. *Anat. Rec. (Hoboken.)* **297**, 1414-1429. doi:10.1002/ar.22949

Anderson, R. H., Jensen, B., Mohun, T. J., Petersen, S. E., Aung, N., Zemrak, F., Planken, R. N. and MacIver, D. H. (2017). Key questions relating to left ventricular noncompaction cardiomyopathy: is the emperor still wearing any clothes? *Can. J. Cardiol.* **33**, 747-757 doi:10.1016/j.cjca.2017.01.017

Anderson, R. H., Spicer, D. E., Mohun, T. J., Hikspoors, J. and Lamers, W. H. (2019). Remodeling of the embryonic interventricular communication in regard to the description and classification of ventricular septal defects. *Anat. Rec. (Hoboken)* **302**, 19-31. doi:10.1002/ar.24020

Asami, I. (1969). Beitrag zur Entwicklung des Kammerseptums im menschlichen Herzen mit besonderer Berücksichtigung der sogenannten Bulbusdrehung. *Zeitschrift für Anatomie und Entwicklungsgeschichte* **128**, 1-17. doi:10.1007/BF00522490

Bakker, M. L., Boukens, B. J., Mommersteeg, M. T., Brons, J. F., Wakker, V., Moorman, A. F. and Christoffels, V. M. (2008). Transcription factor Tbx3 is required for the specification of the atrioventricular conduction system. *Circ. Res.* **102**, 1340-1349. doi:10.1161/CIRCRESAHA.107.169565

Benninghoff, A. (1933). Das Herz. In *Handbuch der vergleichende Anatomie der Wirbeltiere* (ed. L. Bolk, E. Göppert, E. Kallius and W. Lubosch), pp. 467-555. Berlin: Urban & Schwarzenberg.

Boukens, B. J. and Christoffels, V. M. (2012). Electrophysiological patterning of the heart. *Pediatr. Cardiol.* **33**, 900-906. doi:10.1007/s00246-012-0237-4

Brücke, E. (1852). Beiträge zur vergleichenden anatomie und physiologie des Gefäss-systemes. *Denkschriften der kaiserliche Akademie der Wissenschaften - Mathematisch-Naturwissenschaftliche Classe* **3**, 335-367. doi:10.5962/bhl.title.60847

Bruneau, B. G., Logan, M., Davis, N., Levi, T., Tabin, C. J., Seidman, J. G. and Seidman, C. E. (1999). Chamber-specific cardiac expression of Tbx5 and heart defects in Holt-Oram syndrome. *Dev. Biol.* **211**, 100-108. doi:10.1006/dbio.1999.9298

Bruneau, B. G., Nemer, G., Schmitt, J. P., Charron, F., Robitaille, L., Caron, S., Conner, D. A., Gessler, M., Nemer, M., Seidman, C. E. et al. (2001). A murine model of Holt-Oram syndrome defines roles of the T-box transcription factor Tbx5 in cardiogenesis and disease. *Cell* **106**, 709-721. doi:10.1016/S0092-8674(01)00493-7

Burggren, W. W. and Johansen, K. (1982). Ventricular hemodynamics in the monitor lizard Varanus exanthematicus: pulmonary and systemic pressure separation. *J. Exp. Biol.* **96**, 343-354.

Burggren, W. W. and Johansen, K. (1986). Circulation and respiration in lungfishes (Dipnoi). *J. Morph.* **1**, 217-236. doi:10.1002/jmor.1051900415

Captur, G., Syrris, P., Obianyo, C., Limongelli, G. and Moon, J. C. (2015). Formation and malformation of cardiac trabeculae: biological basis, clinical significance, and special yield of magnetic resonance imaging in assessment. *Can. J. Cardiol.* **31**, 1325-1337. doi:10.1016/j.cjca.2015.07.003

Chapman, D. L., Garvey, N., Hancock, S., Alexiou, M., Agulnik, S. I., Gibson-Brown, J. J., Cebra-Thomas, J., Bollag, R. J., Silver, L. M. and Papaioannou, V. E. (1996). Expression of the T-box family genes, Tbx1-Tbx5, during early mouse development. *Dev. Dyn.* **206**, 379-390. doi:10.1002/(SICI)1097-0177(199608)206:4<379::AID-AJA4>3.0.CO;2-F

Christian, E. and Grigg, G. C. (1999). Electrical activation of the ventricular myocardium of the crocodile Crocodylus johnstoni: a combined microscopic and electrophysiological study. *Comp. Biochem. Physiol. A* **123**, 17-23. doi:10.1016/S1095-6433(99)00024-0

Christoffels, V. M., Habets, P. E. M. H., Franco, D., Campione, M., de Jong, F., Lamers, W. H., Bao, Z. Z., Palmer, S., Biben, C., Harvey, R. P. et al. (2000a). Chamber formation and morphogenesis in the developing mammalian heart. *Dev. Biol.* **223**, 266-278. doi:10.1006/dbio.2000.9753

Christoffels, V. M., Keijser, A. G. M., Houweling, A. C., Clout, D. E. W. and Moorman, A. F. M. (2000b). Patterning the embryonic heart: Identification of five mouse Iroquois homeobox genes in the developing heart. *Dev. Biol.* **224**, 263-274. doi:10.1006/dbio.2000.9801

Chuck, E. T., Meyers, K., France, D., Creazzo, T. L. and Morley, G. E. (2004). Transitions in ventricular activation revealed by two-dimensional optical mapping. *Anat. Rec. A Discov. Mol. Cell Evol. Biol.* **280**, 990-1000. doi:10.1002/ar.a.20083

Cook, A. C., Tran, V. H., Spicer, D. E., Rob, J. M. H., Sridharan, S., Taylor, A., Anderson, R. H. and Jensen, B. (2017). Sequential segmental analysis of the crocodilian heart. *J. Anat.* **231**, 484-499. doi:10.1111/joa.12661

de Groot, I., Sanders, E., Visser, S., Lamers, W., de Jong, F., Los, J. and Moorman, A. (1987). Isomyosin expression in developing chicken atria: a marker for the development of conductive tissue? *Anat. Embryol.* **176**, 515-523. doi:10.1007/BF00310091

Durrer, D., van Dam, R. T., Freud, G. E., Janse, M. J., Meijler, F. L. and Arzbaecher, R. C. (1970). Total excitation of the isolated human heart. *Circulation* **41**, 899-912. doi:10.1161/01.CIR.41.6.899

Farmer, C. G. and Sanders, K. (2010). Unidirectional airflow in the lungs of alligators. *Science* **327**, 338-340. doi:10.1126/science.1180219

Finsterer, J., Stöllberger, C. and Towbin, J. A. (2017). Left ventricular noncompaction cardiomyopathy: cardiac, neuromuscular, and genetic factors. *Nat. Rev. Cardiol.* **14**, 224-237. doi:10.1038/nrcardio.2016.207
Gibson-Brown, J. J., Agulnik, S. I., Silver, L. M. and Papaioannou, V. E. (1998). Expression of T-box genes Tbx2-Tbx5 during chick organogenesis. *Mech. Dev.* **74**, 165-169. doi:10.1016/S0925-4773(98)00056-2
Gregorovicova, M., Sedmera, D. and Jensen, B. (2018). Relative position of the atrioventricular canal determines the electrical activation of developing reptile ventricles. *J. Exp. Biol.* **221**, jeb178400. doi:10.1242/jeb.178400
Gregorovicova, M., Zahradnicek, O., Tucker, A. S., Velensky, P. and Horacek, I. (2012). Embryonic development of the monitor lizard, Varanus indicus. *Amphib-Reptilia* **33**, 451-468. doi:10.1163/15685381-00002849
Greil, A. (1903). Beitrage zur vergelichenden anatomie und entwicklungsgeschichte des herzens und des trauncus arteriosus der wirbelthiere. *Morph. Jahrbuch* **31**, 123-310.
Heisler, N. and Glass, M. L. (1985). Mechanisms and regulation of central vascular shunts in reptiles. In *Cardiovascular Shunts* (ed. K. Johansen and W. W. Burggren), pp. 334-353. Munksgaard: Alfred Benzon Symposium 21.
Heisler, N., Neumann, P. and Maloiy, G. M. O. (1983). The mechanism of intracardiac shunting in the lizard *Varanus exanthematicus*. *J. Exp. Biol.* **105**, 15-31.
Hicks, J. W. (1998). Cardiac shunting in reptiles: mechanisms, regulation and physiological functions. In *Morphology G: The Visceral Organs* (ed. C. Gans and A. S. Gaunt), pp. 425-483. Ithaca, New York: Society for the Study of Amphibians and Reptiles.
Hoogaars, W. M. H., Tessari, A., Moorman, A. F. M., de Boer, P. A. J., Hagoort, J., Soufan, A. T., Campione, M. and Christoffels, V. M. (2004). The transcriptional repressor Tbx3 delineates the developing central conduction system of the heart. *Cardiovasc. Res.* **62**, 489-499. doi:10.1016/j.cardiores.2004.01.030
Ishimatsu, A., Hicks, J. W. and Heisler, N. (1988). Analysis of intracardiac shunting in the lizard, *Varanus niloticus*: a new model based on blood oxygen levels and microsphere distribution. *Respir. Physiol.* **71**, 83-100. doi:10.1016/0034-5687(88)90117-X
Jensen, B. (2019). Commemoration of comparative cardiac anatomy of the reptilia I-IV. *J. Morphol.* **280**, 623-626. doi:10.1002/jmor.20964
Jensen, B. and Moorman, A. F. M. (2016). Evolutionary aspects of cardiac development. In *Congenital Heart Diseases: The Broken Heart* (ed. S. Rickert-Sperling, R. Kelly and D. J. Driscoll), pp. 109-117. Springer.
Jensen, B., Nyengaard, J., Pedersen, M. and Wang, T. (2010). Anatomy of the python heart. *Anat. Sci. Int.* **85**, 194-203. doi:10.1007/s12565-010-0079-1
Jensen, B., Boukens, B. J., Postma, A. V., Gunst, Q. D., van den Hoff, M. J., Moorman, A. F., Wang, T. and Christoffels, V. M. (2012). Identifying the evolutionary building blocks of the cardiac conduction system. *PLoS ONE* **7**, e44231. doi:10.1371/journal.pone.0044231
Jensen, B., van den Berg, G., van den Doel, R., Oostra, R. J., Wang, T. and Moorman, A. F. (2013). Development of the hearts of lizards and snakes and perspectives to cardiac evolution. *PLoS ONE* **8**, e63651. doi:10.1371/journal.pone.0063651
Jensen, B., Moorman, A. F. and Wang, T. (2014). Structure and function of the hearts of lizards and snakes. *Biol. Rev. Camb. Philos. Soc.* **89**, 302-336. doi:10.1111/brv.12056
Jensen, B., Boukens, B. J., Crossley, D. A., Conner, J., Mohan, R. A., van Duijvenboden, K., Postma, A. V., Gloschat, C. R., Elsey, R. M., Sedmera, D. et al. (2018). Specialized impulse conduction pathway in the alligator heart. *Elife* **7**, e32120. doi:10.7554/eLife.32120
Joyce, W., Axelsson, M., Altimiras, J. and Wang, T. (2016). In situ cardiac perfusion reveals interspecific variation of intraventricular flow separation in reptiles. *J. Exp. Biol.* **219**, 2220-2227. doi:10.1242/jeb.139543
Koshiba-Takeuchi, K., Mori, A. D., Kaynak, B. L., Cebra-Thomas, J., Sukonnik, T., Georges, R. O., Latham, S., Beck, L., Henkelman, R. M., Black, B. L. et al. (2009). Reptilian heart development and the molecular basis of cardiac chamber evolution. *Nature* **461**, 95-98. doi:10.1038/nature08324
Lamers, W. H., Viragh, S., Wessels, A., Moorman, A. F. and Anderson, R. H. (1995). Formation of the tricuspid valve in the human heart. *Circulation* **91**, 111-121. doi:10.1161/01.CIR.91.1.111
Laurin, M. and Reisz, R. R. (1995). A Reevaluation of Early Amniote Phylogeny. *Zool. J. Linn. Soc.* **113**, 165-223. doi:10.1111/j.1096-3642.1995.tb00932.x
Michaëlsson, M. and Ho, S. Y. (2000). *Congenital Heart Malformations in Mammals*. World Scientific Publishing Company.
Moorman, A. F. M., de Jong, F., Denyn, M. M. and Lamers, W. H. (1998). Development of the cardiac conduction system. *Circ. Res.* **82**, 629-644. doi:10.1161/01.RES.82.6.629
Moorman, A. F., Houweling, A. C., de Boer, P. A. and Christoffels, V. M. (2001). Sensitive nonradioactive detection of mRNA in tissue sections: novel application of the whole-mount in situ hybridization protocol. *J. Histochem. Cytochem.* **49**, 1-8. doi:10.1177/002215540104900101
Perry, S. F. and Sander, M. (2004). Reconstructing the evolution of the respiratory apparatus in tetrapods. *Respir. Physiol. Neurobiol.* **144**, 125-139. doi:10.1016/j.resp.2004.06.018
Poelmann, R. E., Groot, A. C., Vicente-Steijn, R., Wisse, L. J., Bartelings, M. M., Everts, S., Hoppenbrouwers, T., Kruithof, B. P., Jensen, B., de Bruin, P. W. et al. (2014). Evolution and development of ventricular septation in the amniote heart. *PLoS ONE* **9**, e106569. doi:10.1371/journal.pone.0106569
Poelmann, R. E., Gittenberger-de Groot, A. C., Biermans, M. W. M., Dolfing, A. I., Jagessar, A., van Hattum, S., Hoogenboom, A., Wisse, L. J., Vicente-Steijn, R., de Bakker, M. A. G. et al. (2017). Outflow tract septation and the aortic arch system in reptiles: lessons for understanding the mammalian heart. *Evodevo* **8**, 9. doi:10.1186/s13227-017-0072-z
Reckova, M., Rosengarten, C., DeAlmeida, A., Stanley, C. P., Wessels, A., Gourdie, R. G., Thompson, R. P. and Sedmera, D. (2003). Hemodynamics is a key epigenetic factor in development of the cardiac conduction system. *Circ. Res.* **93**, 77-85. doi:10.1161/01.RES.0000079488.91342.B7
Rentschler, S., Vaidya, D. M., Tamaddon, H., Degenhardt, K., Sassoon, D., Morley, G. E., Jalife, J. and Fishman, G. I. (2001). Visualization and functional characterization of the developing murine cardiac conduction system. *Development* **128**, 1785-1792.
Rychterova, V. (1971). Principle of growth in thickness of the heart ventricular wall in the chick embryo. *Folia Morphol. (Praha)* **19**, 262-272.
Sanger, T. J., Losos, J. B. and Gibson-Brown, J. J. (2008). A developmental staging series for the lizard genus Anolis: a new system for the integration of evolution, development, and ecology. *J. Morphol.* **269**, 129-137. doi:10.1002/jmor.10563
Sankova, B., Benes, J., Jr, Krejci, E., Dupays, L., Theveniau-Ruissy, M., Miquerol, L. and Sedmera, D. (2012). The effect of connexin40 deficiency on ventricular conduction system function during development. *Cardiovasc. Res.* **95**, 469-479. doi:10.1093/cvr/cvs210
Schachner, E. R., Cieri, R. L., Butler, J. P. and Farmer, C. G. (2014). Unidirectional pulmonary airflow patterns in the savannah monitor lizard. *Nature* **506**, 367-370. doi:10.1038/nature12871
Sedmera, D., Pexieder, T., Vuillemin, M., Thompson, R. P. and Anderson, R. H. (2000). Developmental patterning of the myocardium. *Anat. Rec.* **258**, 319-337. doi:10.1002/(SICI)1097-0185(20000401)258:4<319::AID-AR1>3.0.CO;2-O
Sedmera, D., Reckova, M., DeAlmeida, A., Sedmerova, M., Biermann, M., Volejnik, J., Sarre, A., Raddatz, E., McCarthy, R. A., Gourdie, R. G. et al. (2003). Functional and morphological evidence for a ventricular conduction system in zebrafish and Xenopus hearts. *Am. J. Physiol. Heart Circ. Physiol.* **284**, H1152-H1160. doi:10.1152/ajpheart.00870.2002
Sizarov, A., Devalla, H. D., Anderson, R. H., Passier, R., Christoffels, V. M. and Moorman, A. F. (2011). Molecular analysis of the patterning of the conduction tissues in the developing human heart. *Circ. Arrhythm. Electrophysiol.* **4**, 532-542. doi:10.1161/CIRCEP.111.963421
Soufan, A. T., Ruijter, J. M., van den Hoff, M. J., de Boer, P. A., Hagoort, J. and Moorman, A. F. (2003). Three-dimensional reconstruction of gene expression patterns during cardiac development. *Physiol. Genomics* **13**, 187-195. doi:10.1152/physiolgenomics.00182.2002
Thompson, G. G. and Withers, P. C. (1997). Standard and maximal metabolic rates of goannas (Squamata:Varanidae). *Physiol. Zool.* **70**, 307-323. doi:10.1086/639605
Van Mierop, L. H. S. and Kutsche, L. M. (1985). Development of the ventricular septum of the heart. *Heart Vessels* **1**, 114-119. doi:10.1007/BF02066358
van Rijen, H. V., van Veen, T. A., van Kempen, M. J., Wilms-Schopman, F. J., Potse, M., Krueger, O., Willecke, K., Opthof, T., Jongsma, H. J. and de Bakker, J. M. (2001). Impaired conduction in the bundle branches of mouse hearts lacking the gap junction protein connexin40. *Circulation* **103**, 1591-1598. doi:10.1161/01.CIR.103.11.1591
Webb, G. J. W. (1979). Comparative cardiac anatomy of the reptilia III. The heart of crocodilians and an hypothesis on the completion of the interventricular septum of crocodilians and birds. *J. Morph.* **161**, 221-240. doi:10.1002/jmor.1051610209
Webb, G., Heatwole, H. and Bavay, J. (1971). Comparative cardiac anatomy of the Reptilia I. The chambers and septa of the varanid ventricle. *J.Morph.* **134**, 335-350. doi:10.1002/jmor.1051340306
Wenink, A. C. G. (1981). Embryology of the ventricular septum-separate origin of its components. *Virchows Arch. A Pathol. Anat. Histopathol.* **390**, 71-79. doi:10.1007/BF00443898
White, F. N. (1959). Circulation in the reptilian heart (Squamata). *Anat. Rec.* **135**, 129-134. doi:10.1002/ar.1091350208
White, F. N. (1968). Functional anatomy of the heart of reptiles. *Am. Zool.* **8**, 211-219. doi:10.1093/icb/8.2.211
Yamada, M., Revelli, J. P., Eichele, G., Barron, M. and Schwartz, R. J. (2000). Expression of chick Tbx-2, Tbx-3, and Tbx-5 genes during early heart development: evidence for BMP2 induction of Tbx2. *Dev. Biol.* **228**, 95-105. doi:10.1006/dbio.2000.9927
Yutzey, K. E., Rhee, J. T. and Bader, D. (1994). Expression of the atrial-specific myosin heavy chain AMHC1 and the establishment of anteroposterior polarity in the developing chicken heart. *Development* **120**, 871-883.